

**Zeitschrift:** IABSE publications = Mémoires AIPC = IVBH Abhandlungen  
**Band:** 22 (1962)

**Artikel:** Ultimate strength of high yield strength constructional-alloy circular columns: effect of cold straightening  
**Autor:** Nitta, Akira / Thürlmann, Bruno  
**DOI:** <https://doi.org/10.5169/seals-18811>

#### **Nutzungsbedingungen**

Die ETH-Bibliothek ist die Anbieterin der digitalisierten Zeitschriften auf E-Periodica. Sie besitzt keine Urheberrechte an den Zeitschriften und ist nicht verantwortlich für deren Inhalte. Die Rechte liegen in der Regel bei den Herausgebern beziehungsweise den externen Rechteinhabern. Das Veröffentlichen von Bildern in Print- und Online-Publikationen sowie auf Social Media-Kanälen oder Webseiten ist nur mit vorheriger Genehmigung der Rechteinhaber erlaubt. [Mehr erfahren](#)

#### **Conditions d'utilisation**

L'ETH Library est le fournisseur des revues numérisées. Elle ne détient aucun droit d'auteur sur les revues et n'est pas responsable de leur contenu. En règle générale, les droits sont détenus par les éditeurs ou les détenteurs de droits externes. La reproduction d'images dans des publications imprimées ou en ligne ainsi que sur des canaux de médias sociaux ou des sites web n'est autorisée qu'avec l'accord préalable des détenteurs des droits. [En savoir plus](#)

#### **Terms of use**

The ETH Library is the provider of the digitised journals. It does not own any copyrights to the journals and is not responsible for their content. The rights usually lie with the publishers or the external rights holders. Publishing images in print and online publications, as well as on social media channels or websites, is only permitted with the prior consent of the rights holders. [Find out more](#)

**Download PDF:** 17.01.2026

**ETH-Bibliothek Zürich, E-Periodica, <https://www.e-periodica.ch>**

# Ultimate Strength of High-Yield Strength Constructional-Alloy Circular Columns — Effect of Cold-Straightening

*Résistance limite des barres comprimées à section circulaire, en alliage à haute limite élastique — Influence du dressage à froid*

*Tragfähigkeit von Säulen mit Kreisquerschnitt aus legiertem Baustahl mit hoher Fließgrenze — Einfluß des Kalt-Richtens*

AKIRA NITTA

National Aeronautical Laboratory,  
Tokyo\*)

BRUNO THÜRLIMANN

Swiss Federal Institute of Technology,  
Zurich\*)

## I. Introduction

Rolled steel sections are usually straightened by such operations as cold-bending, gagging, rotarizing, etc. Since these operations involve plastic deformations of the material, residual stresses will be introduced into the members. For rolled wide-flange columns HUBER [1]<sup>1)</sup> investigated this problem and showed that the secant formula may lead to unconservative results for medium length columns. However, the reported test data are insufficient to allow conclusions for more general cases. The ultimate strength of columns failing in the inelastic range depends markedly on the magnitude and distribution of the residual stresses. They, in turn, depend on the shape of the cross section and on the amount of straightening. It should be emphasized that in practical cases a variety of fairly large initial curvatures (e.g. kinks or knuckles) will exist in rolled column members prior to cold-straightening and small residual curvatures will exist even after straightening.

When circular heat-treated column members are cold-straightened, two kinds of residual stresses, namely thermal and cold-bending residual stresses, co-exist in the material. Due to the triaxiality of the thermal residual stresses in such members the formation of the secondary residual stresses caused by the cold-straightening operation will be so complicated that a general ana-

<sup>\*</sup>) Formerly Fritz Engineering Laboratory Lehigh University, Bethlehem, Pa.

<sup>1)</sup> The numbers in parentheses refer to the list of references.

lytical approach for obtaining the final residual stress distribution would be extremely difficult, although the residual stresses caused by either cooling or by cold-straightening can be predicted theoretically. Practical straightening processes often would result in localized residual stresses at certain locations or in stresses varying along the member, but for simplicity, the worst case, that of uniform residual stress along the entire member, will be considered in this paper. An experimental method to determine such non-polar symmetric residual stresses in circular cylinders was suggested by LAMBERT [2]. His method, the "modified boring-out method", seems suitable for application to the present case with a modification to be discussed subsequently.

A general method for analysing the ultimate strength of high-yield strength alloy steel circular columns as influenced by the presence of thermal residual stresses was presented by the authors in Reference [3]. As an extension of this work, the effect of anti-symmetric residual stresses due to cold-straightening and the small out-of-straightness remaining after cold-straightening on the ultimate load-carrying capacity of column members will be discussed in this paper.

To verify these theories, constructional alloy and structural carbon steel bars having a uniform curvature (out-of-straightness) were cold-straightened in the laboratory and some bars were subsequently stress relieved. Residual stress measurements and stub column tests were made on bars (1) before straightening, (2) after straightening and (3) after stress relieving. Column tests were performed on (1) cold-straightened and (2) stress relieved (after cold-straightening) bars.

## II. Cold-Straightening of Beams

An initially curved column member can be straightened by an application of load which causes the same amount of permanent deformations in the reverse direction. Since the initial deflected shape of actual members may be rather arbitrary, the final shape will not be perfectly straight unless an appropriate system of multi-point loading is used. As a matter of fact, a method called

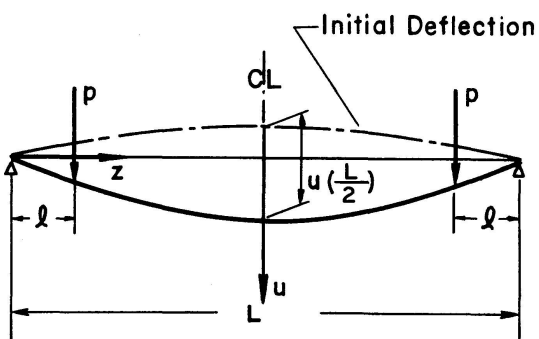


Fig. 1. Cold-straightening of column members.

“gagging” is frequently used in mill practice to straighten steel members within some allowable tolerance. This operation applies a “three-point loading” (one concentrated load between two supports) at various initially curved portions of the specimen. However, for the current investigation it was found more convenient to use a four-point loading system (two concentrated loads between two supports, Fig. 1) to straighten the specimens. In this way a column specimen containing uniformly distributed residual stresses along the entire length was obtained.

A theoretical analysis of the load-deflection relationship of the specimen subjected to cold-bending was made before the test to predict the loads required to straighten the specimens.

Since this analysis covers the general “four-point loading system”, which includes the “three-point loading system” as a special case, the results of the solution will provide basic information on the cold-straightening of column members.

### 1. Theoretical Load-Deflection Relationship and Residual Stresses

By using the simple plastic theory [4] applied to the problem of the flexure of a beam with circular cross section, a load-deflection analysis is conducted for a simply supported beam (length  $L$ ) which is subjected to two equal loads, each load  $p$  being at a distance  $l$  from the end of the beam. (See Appendix A.) This analysis shows that the deflection at the center of the beam,  $\mu(L/2)$ , can be expressed by the following formula in terms of  $\beta$  ( $\equiv M_0/M_p$ ), the ratio of the cold-bending moment  $M_0$  to the full plastic moment  $M_p$ .

$$\frac{u(L/2)}{u^*} = \frac{9\pi}{8} \frac{\gamma^2}{\beta^2(3-\gamma^2)} \left[ \frac{3\pi^2}{256} + \frac{1}{2} \beta^2 \left( \frac{1}{\gamma^2} - 1 \right) F(\beta) + \beta F_1(\beta) - F_2(\beta) \right], \quad (1)$$

where  $\gamma \equiv \frac{l}{L/2}$   $u^* = \frac{M_p L^2}{24 EI} (3 - \gamma^2)$

elastic deflection at the center when the beam is subjected to a moment equal to  $M_p$ .

Through numerical integration the functions  $F(\beta)$ ,  $F_1(\beta)$  and  $F_2(\beta)$  were computed for various values of  $\beta$ , and are illustrated by the curves in Fig. 2.

When the beam is completely unloaded after applying the load  $p$ , the residual deflection  $\bar{u}$  will be obtained by subtracting the elastic deflection  $\bar{u}_e$  (caused by load  $p$ ) from the one given by Eq. (1).

$$\bar{u} = u - u_e. \quad (2)$$

A uniformly curved beam, of which the initial deflection at the center is equal to  $\delta$ , can be straightened by applying a bending moment  $\beta$  which produces the same amount of residual deflection (given by Eq. (2)) as  $\delta$ . Since

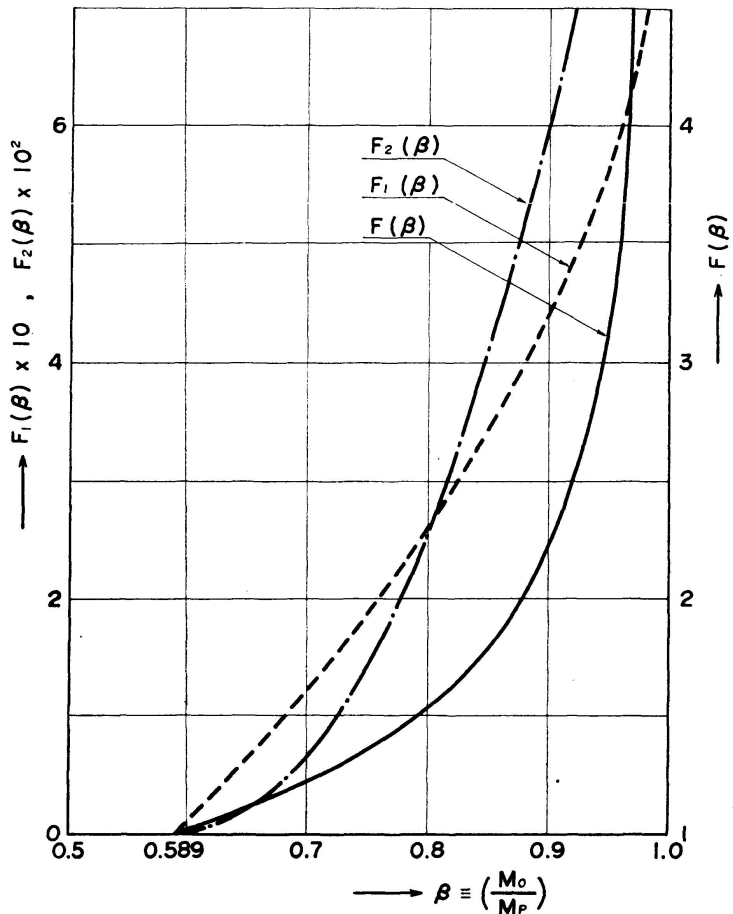


Fig. 2. Functions  $F(\beta)$ ,  $F_1(\beta)$  and  $F_2(\beta)$ .

$$\frac{u_e(L/2)}{u^*} = \frac{M_0}{M_p} = \beta \quad (3)$$

it follows that

$$\delta = u(L/2) - \beta u^* \quad (4)$$

Fig. 3 illustrates the relationship between initial deflections  $\delta$  and the required cold-bending moment  $\beta$  for several values of the parameter  $\gamma$ . It can be seen from this figure that the moment required to straighten a given beam decreases as the parameter  $\gamma$  decreases, the required moment being largest for a three point loading system where  $\gamma = 1$ . Thus, straightening with a four-point system is less likely to cause a plastic hinge in the beam than straightening with a three-point system.

When pre-existing residual stresses caused by heat treatment are neglected<sup>2)</sup>, the distribution of the residual stresses due to the cold-straightening is the sum of the stress produced by the loading at the maximum moment  $M_0$  and the stress which corresponds to the unloading process, assuming elastic behavior

<sup>2)</sup> For material air-cooled from the tempering temperature, the normal production practice, these thermal residual stresses are small.

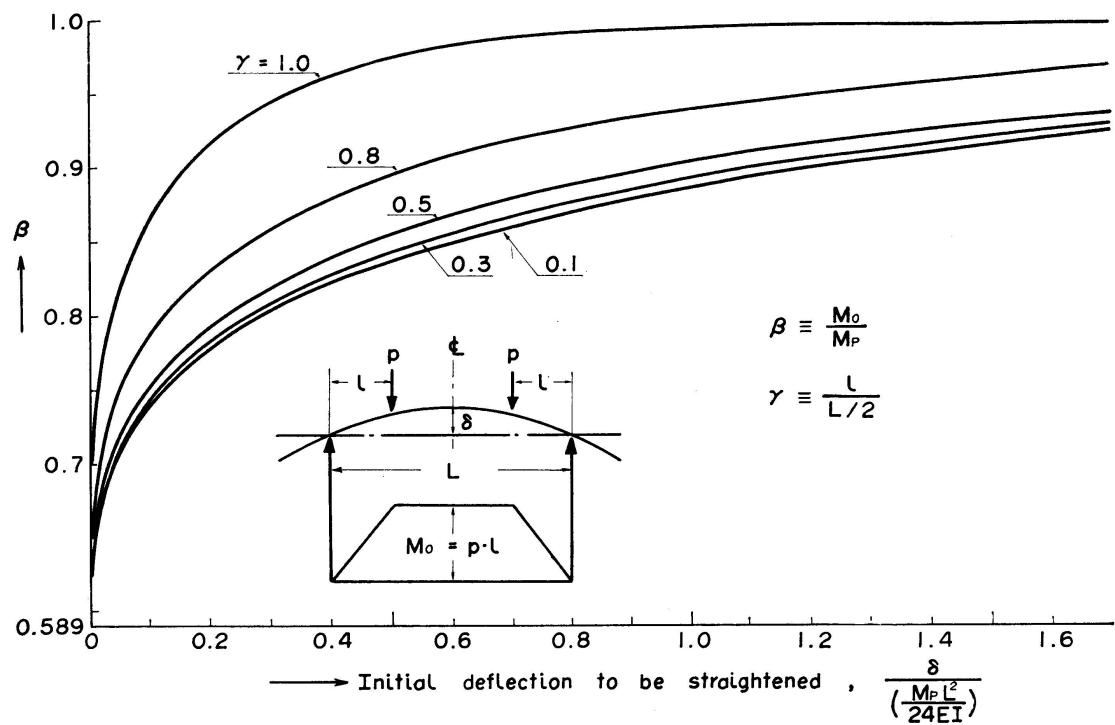


Fig. 3. Initial deflection and required bending moment for cold-straightening.

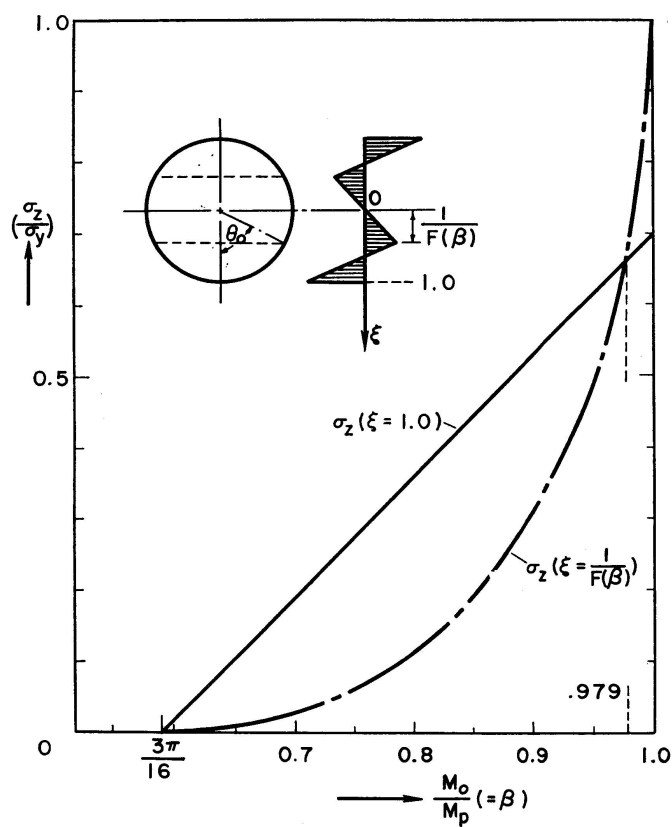


Fig. 4. Residual stress resulting in cold-straightened members.

during unloading. Hence, the axial residual stress,  $\sigma_z$  at a distance  $x$  from the bending axis is given by:

$$\begin{aligned}\frac{\sigma_z(\xi)}{\sigma_y} &= \frac{16}{3\pi} \beta \xi + 1, & \left( \text{for } -1 \leq \xi \leq -\frac{1}{F(\beta)} \right), \\ &= \frac{16}{3\pi} \beta \xi - F(\beta) \xi, & \left( \text{for } -\frac{1}{F(\beta)} \leq \xi \leq \frac{1}{F(\beta)} \right), \\ &= \frac{16}{3\pi} \beta \xi - 1, & \left( \text{for } \frac{1}{F(\beta)} \leq \xi \leq 1 \right),\end{aligned}\quad (5)$$

where  $\sigma_y$  is yield stress of the material, and  $\xi = x/R$ .

The maximum stress occurs at the extreme fiber of the cross section,  $\xi = +1$ , or at  $\xi = +\frac{1}{F(\beta)}$  depending upon the value of the applied bending moment  $\beta$ .

Fig. 4 shows the relationship between the maximum residual stress due to cold-straightening and the applied straightening moment. By using this result together with the  $\delta$  vs  $\beta$  curves in Fig. 3, one can directly estimate the maximum probable value of residual stress in a column specimen straightened by cold-bending provided the magnitude of its initial out-of-straightness,  $\delta$ , is known.

## 2. Cold-Straightening Tests

The eight specimens for use in subsequent tests were cold-straightened in the laboratory. These specimens were USS "T-1" constructional alloy steel and AISI 1020 carbon steel round bars of  $2\frac{3}{4}$  inch diameter, with approximately five inches<sup>3)</sup> of maximum initial deflection within a fifteen foot length. The general set-up of the specimen in the machine used for straightening is illustrated by Fig. 5a and b. It should be pointed out that the tests were conducted in such a way that, regardless of the extremely large amount of deflection at the maximum load, no significant longitudinal frictional forces at the supports were produced. Such forces would have introduced unknown bending moments in the beam. A check was made by comparing the moment-deflection relationship obtained from the measurements with the theoretical curve in Fig. 6. This procedure assured that the beam was straightened within acceptable limits for the column test specimens and that the value of  $\beta$  was known.

<sup>3)</sup> A controlled amount of out-of-straightness was achieved in the "T-1" steel bars by cold-bending after quenching and subsequently tempering and air cooling from the tempering temperature. The carbon steel bars were cold-bent and subsequently stress relieved to produce the desired out-of-straightness. For critical applications, such as compression members in television towers, "T-1" steel bars are normally stress-relieved after cold-straightening.

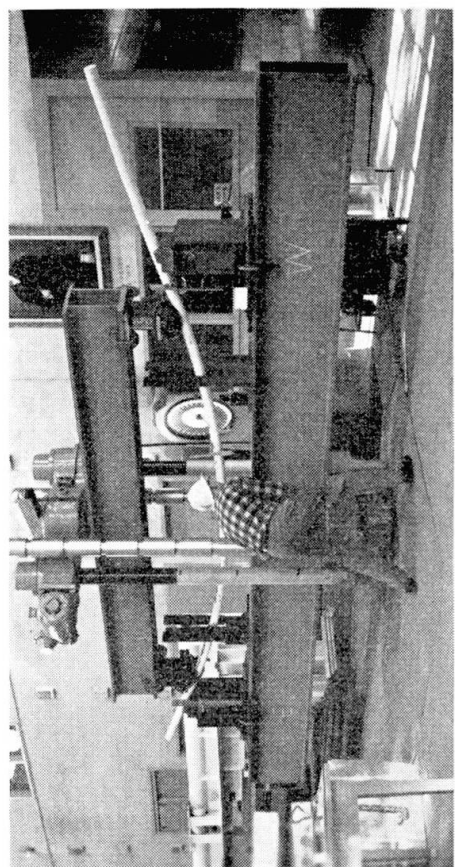
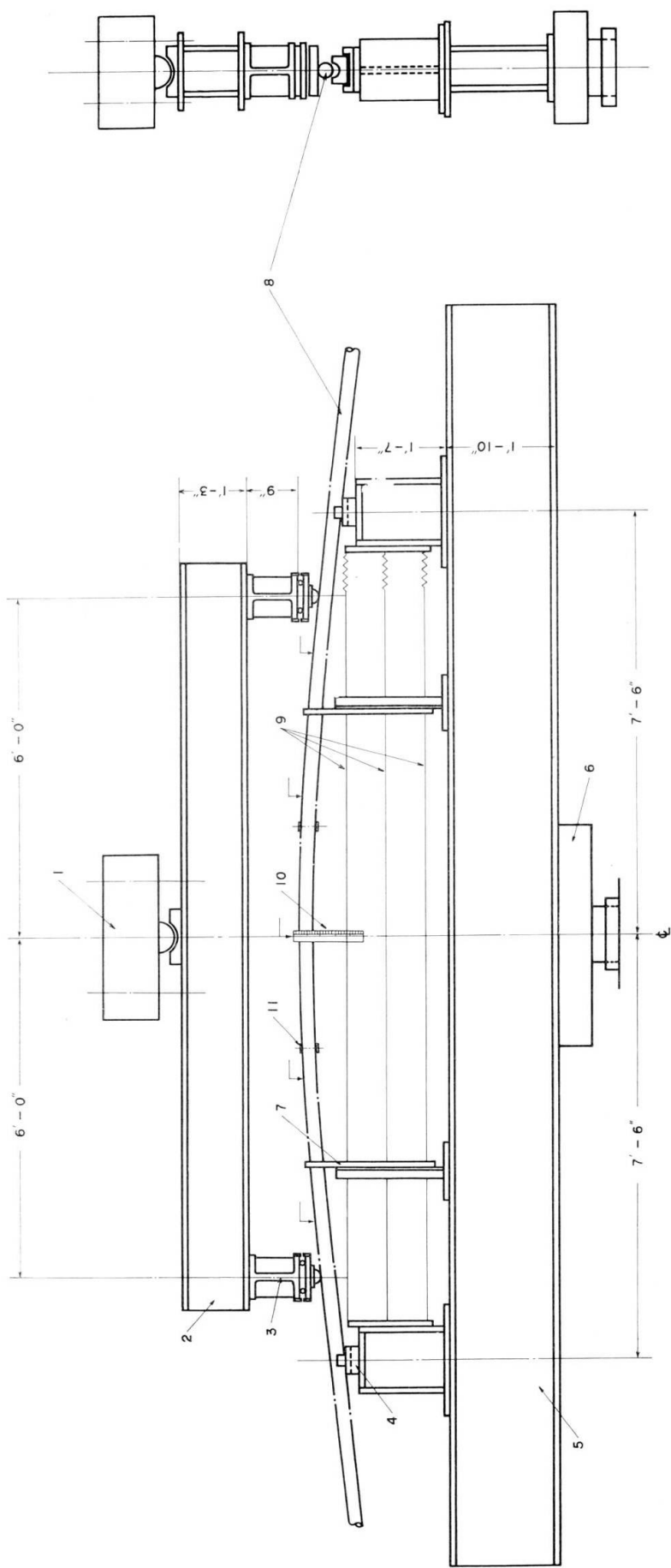


Fig. 5 a and b. Cold-straightening set-up.

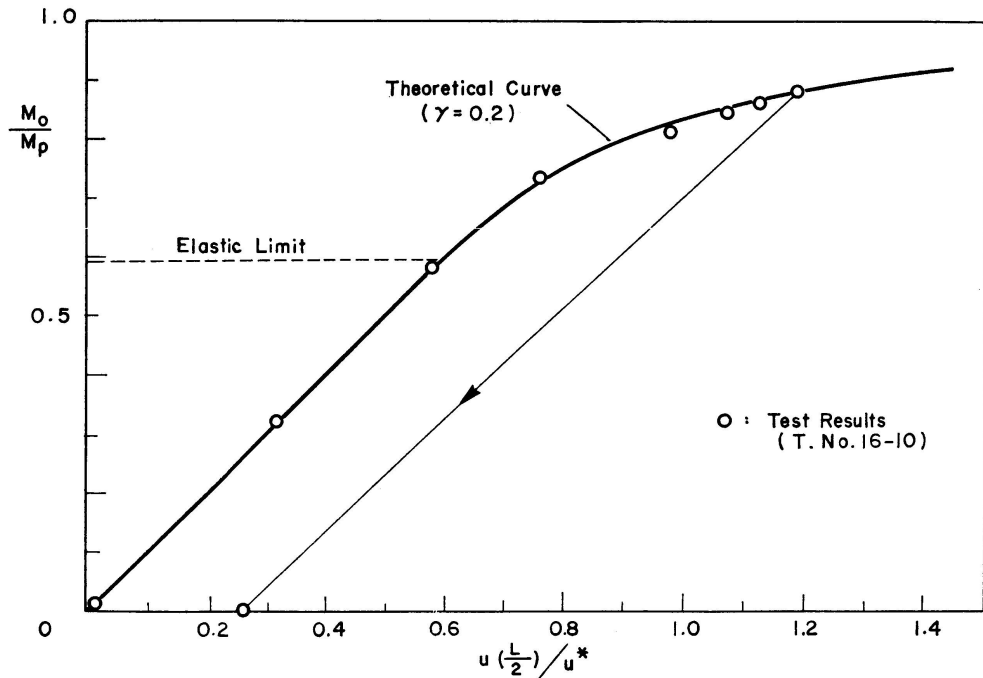


Fig. 6. Moment-deflection diagram.

### III. Measurements of Residual Stresses Caused by Cold-Bending

#### 1. Modified Boring-Out Method

The strains,  $\epsilon$ , which were relaxed by successive boring-out and were measured at four positions on the outside surface of the specimen (see Fig. 7a), are separated into a symmetric set,  $\epsilon_0$  (the average strain of four readings), and an anti-symmetric set,  $\bar{\epsilon}$ .

$$\epsilon = \epsilon_0 + \bar{\epsilon}.$$

The symmetric part can be converted into a symmetric set of residual stresses by the ordinary Sachs equations. The anti-symmetric part of strain in the axial direction, on the other hand, will be related to the anti-symmetric residual stress,  $\sigma_z$ , by the following Volterra's integral equation of the first kind. (See Appendix B.)

$$S(\bar{\rho}) = \int_0^{\bar{\rho}} \sigma_z(\bar{\xi}) K(\bar{\rho}; \bar{\xi}) d\bar{\xi}, \quad (6)$$

where

$$\bar{\rho} \equiv \left( \frac{r}{R} \right)^2 \quad \bar{\xi} \equiv \left( \frac{x}{R} \right)^2,$$

$$S(\bar{\rho}) = \frac{\pi}{8} E (1 - \bar{\rho}^2) \bar{\epsilon}(\bar{\rho}), \quad K(\bar{\rho}; \bar{\xi}) = \sqrt{\bar{\rho} - \bar{\xi}}.$$

Using MacLaurin's expansion method, the residual stress in question at  $\bar{\xi}_i = (i-1) \frac{1}{N}$  is obtained successively from  $i=1$  to  $i=N$  by the following formula,  $N$  being the number of divisions for  $\bar{\xi}$ .

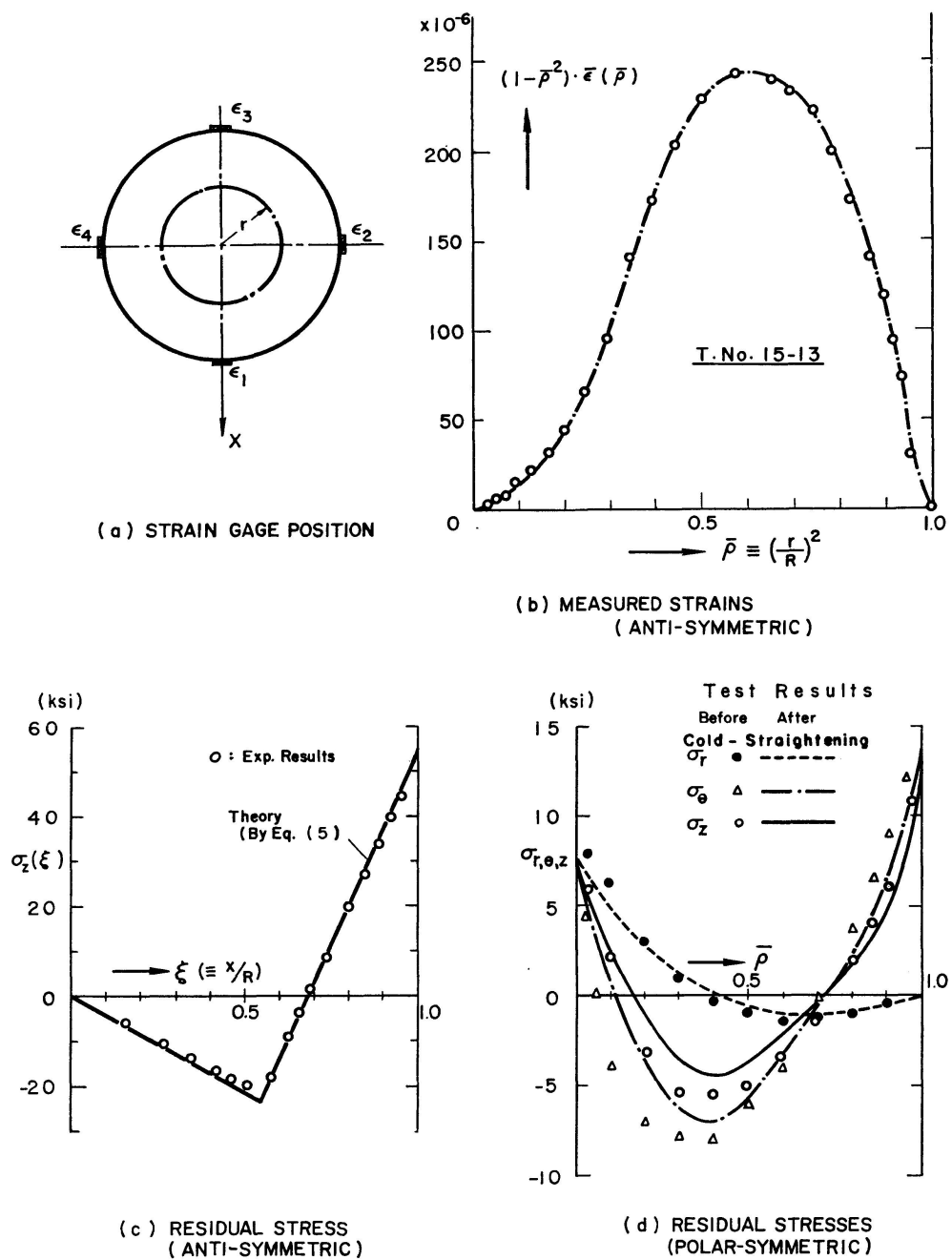


Fig. 7 a), b), c), d). Modified boring-out method.

$$\sigma_z \left( \bar{\rho} \right) = \frac{\frac{S \left( \frac{i}{N} \right)}{\left( \frac{i}{N} \right)} - \sum_{j=1}^{i-1} \alpha_{ij} K \left( \frac{i}{N}; j - \frac{1}{2} \frac{1}{N} \right) \sigma_z \left( j - \frac{1}{2} \frac{1}{N} \right)}{\alpha_{ii} K \left( \frac{i}{N}; i - \frac{1}{2} \frac{1}{N} \right)}, \quad (7)$$

$$(i = 1, 2, \dots, N)$$

where,  $\alpha_{ij}$  are MacLaurin's coefficients given in Appendix B. From a practical point of view it is preferable to first divide the whole region of  $\bar{\xi}$  (from  $\bar{\xi} = 0$

to  $\bar{\xi} = 1$ ) into few parts, and then, subdivide these parts into  $N$  divisions (e.g.  $N = 5$ ) by applying a formula similar to Eq. (7).

Fig. 7c shows an example of the residual stress distribution (anti-symmetric part) obtained by this method, using experimental data of  $\bar{\epsilon}$  (given in Fig. 7b) measured from a cold-straightened specimen [5]. This is compared with theoretical results obtained from Eq. (5) without taking into account the effect of the thermal residual stresses in the specimen. The symmetric part of the residual stresses has also been obtained from the same test specimen by the ordinary Sachs method, and is given in Fig. 7d. In the same figure residual stress distributions in a specimen measured prior to the cold-straightening operation are shown for the purpose of comparison. It can be seen that almost the same amount of residual stress has been found in these two specimens. It is of course true that in steel beams, which initially contained residual stresses due to heat treatment and then were subjected to a cold-straightening operation, the final residual stress is not equal to the superposition of the two stresses produced by heat treatment and cold-bending separately. In other words, the anti-symmetric part of the final residual stresses obtained by this "modified boring-out method" theoretically does not correspond to the one which had been produced by cold-straightening only, without including the pre-existing stresses. However, if the pre-existing stresses are considerably lower than the ones caused by cold-straightening the influence of the former becomes minor. This fact is indicated in Fig. 7c.

## 2. "Beam Dissection Method"

The "modified boring-out method" which takes into account the tri-axiality of residual stresses is quite general, complete and useful, but it involves a considerable amount of work to complete the successive drillings. Therefore it is worthwhile to develop a simpler method of residual stress measurement which can furnish a practical accuracy. If the effects of both the tangential

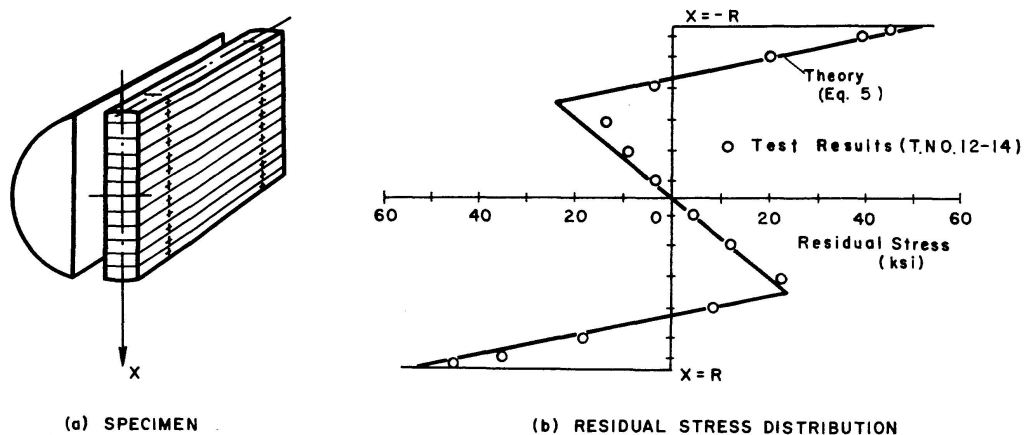


Fig. 8a), b). Beam-dissection method.

and radial components of residual stress in a solid cylinder can be neglected, the beam dissection method is a suitable way of finding the magnitude and distribution of axial residual stresses. The method consists of two steps: 1. cutting a flat piece of plate from the middle part of the round bar in the plane of cold-straightening and, 2. slicing this plate into narrow strips. The change of length within a certain gage length is measured before and after the cutting and the slicing. (See Fig. 8 a.) Residual stresses in  $2\frac{3}{4}$  inch round "T-1" steel bars obtained by this method are shown in Fig. 8 b. Even though this method is only approximate, satisfactory results for use in predicting column strength have been obtained from the tests.

#### IV. Compressive Strength of Cold-Straightened Members

##### 1. Stub Column Tests

The stub column tests were carried out [5] for the following purposes:

1. to indicate the overall effect of the cold-straightening residual stress on compressive members, and 2. to check the effectiveness of stress-relieving.

Fig. 9 shows an example of the stub column test results compared with a theoretical curve for the average stress-strain relationship of a very short column which was subjected to a cold-straightening moment  $\beta = 0.883$ . For three different bars, that is, non-cold-straightened, cold-straightened, and stress-relieved (after being cold-straightened) steels, comparisons are made in terms of the tangent modulus  $E_t$  versus average-stress relationship. (See Fig. 10.) It can be seen that, for both "T-1" steel and carbon steel specimens, stress-relieving was remarkably effective for restoring the tangent modulus to the level of the original material prior to the cold-straightening.

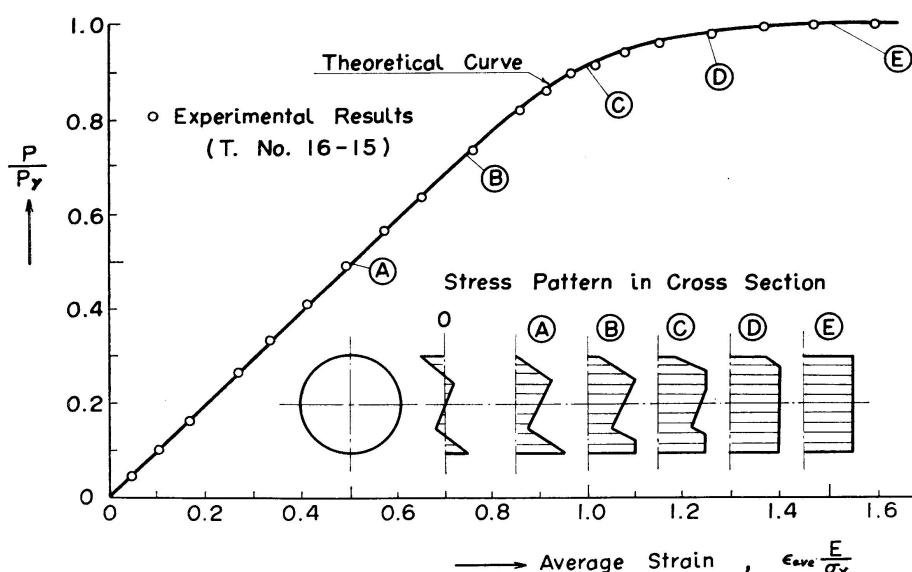


Fig. 9. Average stress-strain curve of stub column.

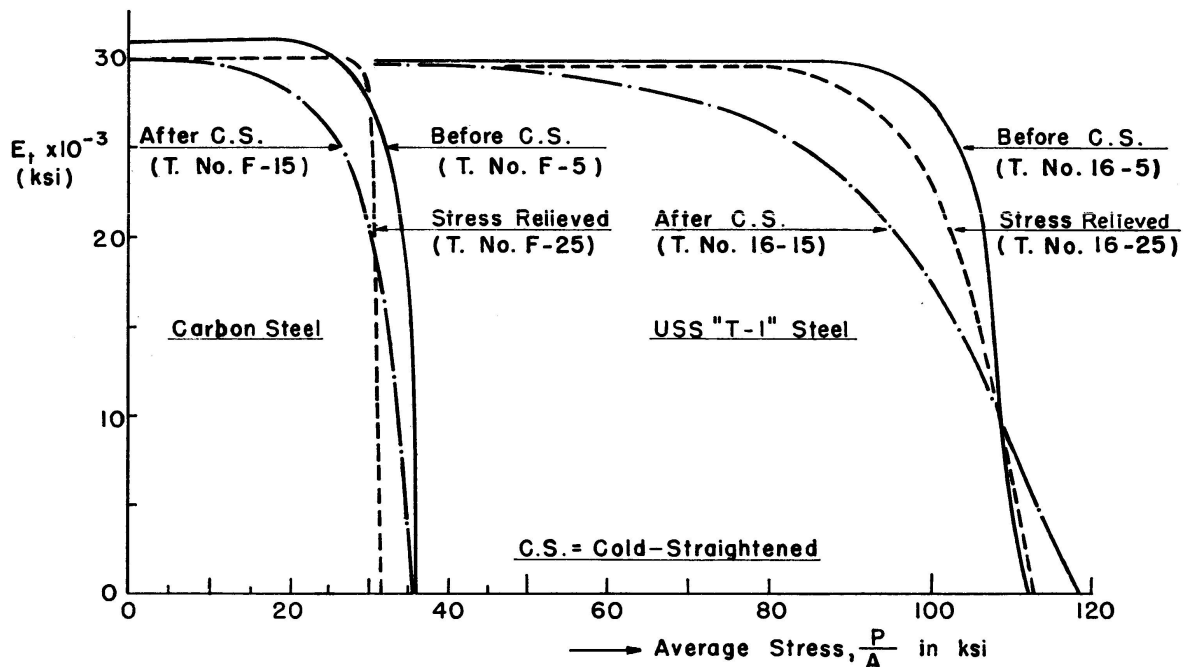


Fig. 10. Effect of both cold-straightening and stress-relieving on tangent modulus of stub column.

## 2. Theoretical Ultimate Strength of Cold-Straightened Columns

A general theoretical analysis of the ultimate strength of high-yield-strength alloy steel circular columns influenced by the presence of residual stresses and initial out-of-straightness of the members has been reported in Ref. [3]. Columns subjected to cold-straightening contain residual stresses of an anti-symmetric pattern with respect to the axis of cold-straightening. If only this kind of residual stress, which is uniaxial, is considered (without including the thermal residual stresses) the equivalent residual stress defined in the previous paper is identical with  $\sigma_z$  given by Eq. (5). Assuming that members have been cold-straightened by an application of a uniform bending moment  $M_0$ , the problem will be limited to a case where the residual stresses are uniformly distributed along the axis of the column. It will be also assumed that the bending of the column under axial thrust is restricted to take place around the axis of cold-bending. Such deformations will be true only when the principal plane of initial deflections coincides with that of the cold-straightening. It should be pointed out, however, that the following two extreme cases will give the upper and the lower limits of the load carrying capacity of the column respectively: 1. the convex side of the initial deflection contains compressive residual stress due to cold-straightening, 2. the convex side contains tensile residual stress.

When such a member is subjected to a concentrically applied axial thrust, it will remain fully elastic if the following relationship is satisfied.

$$0 \leq \lambda \leq 2 - \frac{16}{3\pi}\beta - \varphi,$$

where

$$\lambda \equiv \frac{\sigma_0}{\sigma_y},$$

$\sigma_0$  being the stress at the center of cross section, and

$$\varphi \equiv \frac{E R}{\sigma_y} \Phi.$$

If the column is compressed beyond this elastic limit possible yield patterns will be as shown in Fig. 11. The parameters,  $\theta_1$ ,  $\theta_2$  and  $\theta_3$  are determined as

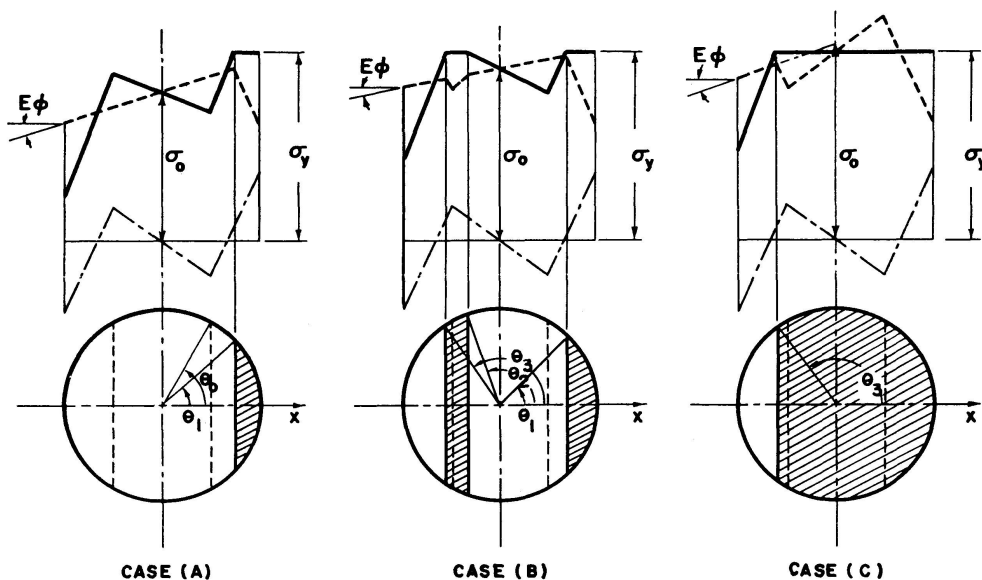


Fig. 11. Yield pattern and stress distribution in cold-straightened columns.

follows. Elastic-plastic case (A):

$$\left(2 - \frac{16}{3\pi}\beta - \varphi\right) \leq \lambda \leq \frac{1}{F(\beta)} \left(\frac{16}{3\pi}\beta + \varphi\right) \quad \theta, (\lambda, \varphi) = \cos^{-1} \left[ \frac{2 - \lambda}{\frac{16}{3\pi}\beta + \varphi} \right]. \quad (8)$$

Elastic-plastic case (B):

$$\frac{1}{F(\beta)} \left(\frac{16}{3\pi}\beta + \varphi\right) \leq \lambda \leq 2 - \frac{1}{F(\beta)} \left(\frac{16}{3\pi}\beta + \varphi\right)$$

$\theta_1$  is given by Eq. (8),

$$\theta_2(\lambda, \varphi) = \cos^{-1} \left[ \frac{1 - \lambda}{\frac{16}{3\pi}\beta - F(\beta) + \varphi} \right], \quad (9)$$

$$\theta_3(\lambda, \varphi) = \cos^{-1} \left[ \frac{-\lambda}{\frac{16}{3\pi}\beta + \varphi} \right]. \quad (10)$$

Elastic-plastic (C):

$$2 - \frac{1}{F(\beta)} \left( \frac{16}{3\pi} \beta + \varphi \right) \leq \lambda \leq \left( \frac{16}{3\pi} \beta + \varphi \right),$$

$\theta_3$  is given by Eq. (10).

Using the basic Eqs. (43') and (44') of Ref. [3], the final expressions for  $P/P_y$  and  $M/P_y R$  are given for each case:

$$\frac{P}{P_y} = U(\lambda, \varphi) = \lambda - \frac{1}{\pi} \left\{ \begin{bmatrix} [(\lambda-2) X_1] \\ [(\lambda-2) X_1 - (\lambda-1) X_2 + \lambda X_3 + X_0] \\ [\lambda X_3] \end{bmatrix} \right. \\ \left. - \frac{2}{3\pi} \left( \frac{16}{3\pi} \beta + \varphi \right) \begin{bmatrix} [Y_1] \\ [Y_1 - Y_2 + Y_3] \\ [Y_3] \end{bmatrix} + \begin{bmatrix} [0] \\ [1 - \frac{2}{3\pi} F(\beta) (Y_2 - Y_0)] \\ [1] \end{bmatrix} \right\}, \quad (11)$$

$$\frac{M}{P_y R} = V(\lambda, \varphi) = \frac{\varphi}{4} - \frac{2}{3\pi} \left\{ \begin{bmatrix} [(\lambda-2) Y_1] \\ [(\lambda-2) Y_1 - (\lambda-1) Y_2 + \lambda Y_3 - Y_0] \\ [\lambda Y_3] \end{bmatrix} \right. \\ \left. - \frac{1}{4\pi} \left( \frac{16}{3\pi} \beta + \varphi \right) \begin{bmatrix} [Z_1] \\ [Z_1 - Z_2 + Z_3] \\ [Z_3] \end{bmatrix} + \begin{bmatrix} [0] \\ \left[ -\frac{1}{4\pi} F(\beta) (Z_2 + Z_0 - \pi) \right] \\ \left[ \frac{4}{3\pi} \beta \right] \end{bmatrix} \right\}, \quad (12)$$

where

$$\begin{aligned} X_i &= \theta_i - \frac{1}{2} \sin(2\theta_i), \\ Y_i &= \sin^3 \theta_i, \\ Z_i &= \theta_i - \frac{1}{4} \sin(4\theta_i), \quad (i = 0, 1, 2, \text{ and } 3). \\ \theta_0 &= \cos^{-1} \left( \frac{1}{F(\beta)} \right), \end{aligned}$$

The upper term in brackets, {}, applies for Case (A), the middle for Case (B) and the lower for Case (C).

By using a method similar to the one described in a previous paper [3], the load-deflection curves can be obtained for the given values of  $\beta$ . A typical example of such a curve is shown in Fig. 12. As can be seen from this figure, a perfectly straight column ( $d_0/R = 0$ ) with anti-symmetric residual stresses starts to deflect at the initiation of yielding (at point *A* in the figure), in the “positive direction” specified as the side where tensile residual stresses are locked-in. As the load increases, the deflection increases to some extent; however, it starts to decrease at point *B*, and returns to a straight configuration when the load is equal to  $P_c$ , whose magnitude depends upon the value of  $\beta$  only. Then the member deflects in the reverse direction — the “negative direction” — and reaches the maximum load,  $P_{max}$ . It was found from the computations that such a reversal of deflection can happen only in short

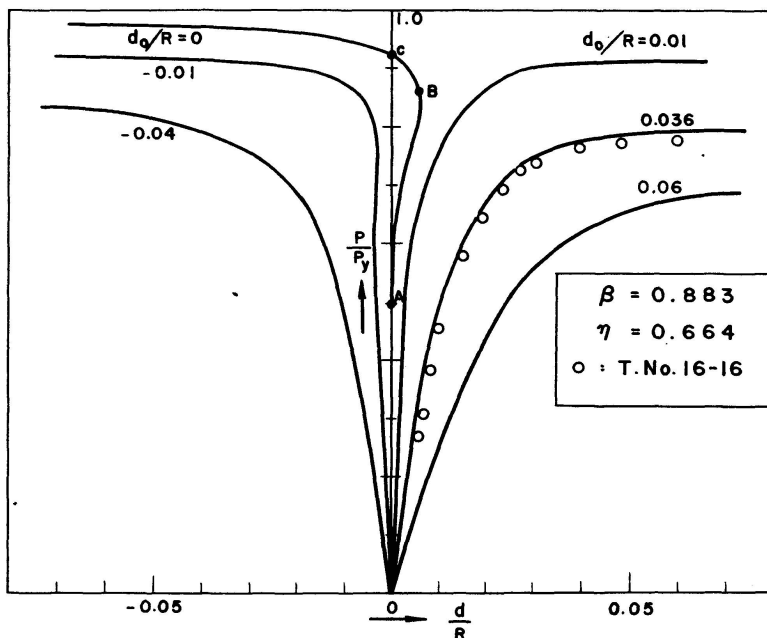


Fig. 12. Load-deflection curves of axially loaded column (including anti-symmetric residual stress).

columns for which the value of  $P_{max}$  is higher than  $P_c$ . On the other hand, longer columns will deflect monotonically in the "positive direction" and the maximum load will never exceed  $P_c$ . If column members have small amounts of "negative initial deflections" — the convex side contains compressive residual stress — their load-carrying capacity is relatively high, and even higher than the strength of a perfectly straight column in the case of longer members. In general, it has been concluded from this analysis that the ultimate strength of cold-straightened column members with "positive initial deflection" is distinctly lower than that of members with "negative initial deflections". The curves in Fig. 13 illustrate this for the case of  $\beta = 0.883$ .

It can be pointed out that a perfectly straightened column subjected to a monotonically increasing axial thrust starts to deflect laterally as soon as the load reached a value at which first yielding takes place in some fiber of the cross section. With a further application of a load increment, the internal stress distribution corresponding to the additional loading will not be symmetric any more due to the effect of localized yielding. Therefore, such a column member in its "undeflected shape" is generally not in a balanced condition with respect to the internal and external moments. Hence the "bent configuration" is the only possible state which satisfies the equilibrium condition. Consequently, no bifurcation point occurs on the load-deflection curve and thus the behavior of columns containing anti-symmetric residual stresses can not be treated as an Eigen-value problem. Consequently the "tangent modulus concept" is not applicable for the prediction of the critical load of cold-straightened columns.

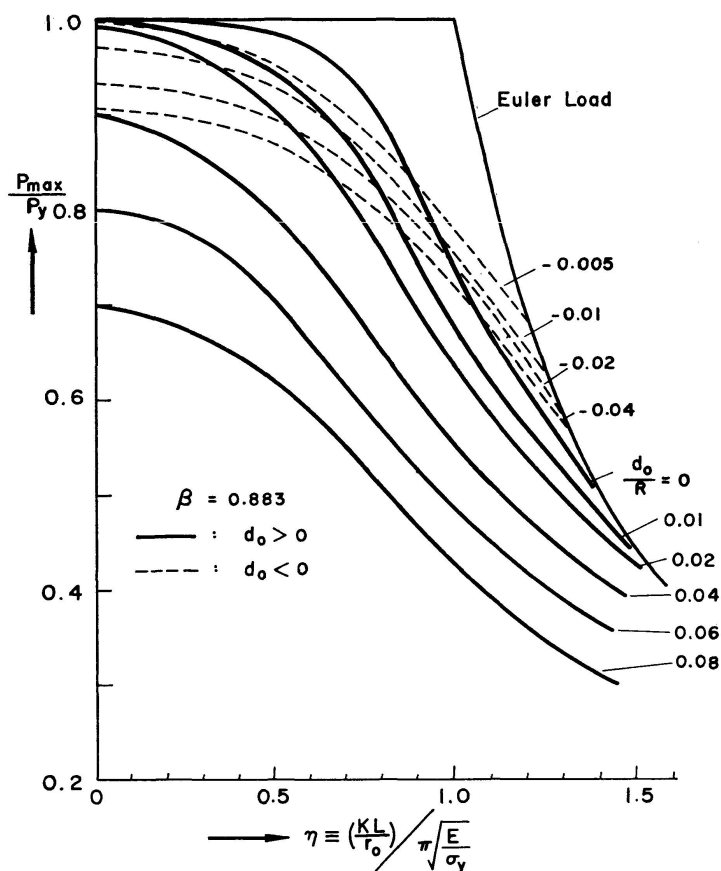


Fig. 13. Ultimate strength of cold-straightened columns.

Table 1. Comparison Between Theory and Test Results on the Ultimate Strength of Columns

Test No.		Length L (in)	Generalized Slenderness Ratio, $\eta$	Initial Deflection After Straightening $d_0/R$	Theory $P_{max}/P_y$	Test $P_{max}/P_y$
A	12—26	40	0.675	0.010	0.95	0.941
	16—26	50.5	0.729	0.065	0.74	0.726
B	12—17	62	1.100	0.025	0.57	0.600
	13—16	40	0.618	0.011	0.91	0.918
	16—16	40	0.664	0.036	0.76	0.773
	F—16*	65	0.665	0.007	0.92	0.922

Group A: Stress-relieved (after straightening) specimens (low residual stress)

Group B: Cold-straightened specimens (high residual stress)

\*: Carbon steel column

### 3. Experimental Ultimate Strength of Cold-Straightened Columns

In order to verify these theoretical predictions, concentrically loaded column tests were carried out on  $2\frac{3}{4}$  inch diameter round specimens of USS "T-1" steel and structural carbon steel [5]. In Fig. 12 are plotted typical results obtained on a specimen with an initial deflection of  $d_0/R = 0.036$ . Table 1 summarizes the column test results and lists the theoretical predictions of their ultimate strength. It can be noted that correlation is fairly good for both cold-straightened and stress-relieved columns.

## V. Summary

1. The relationship between the initial out-of-straightness of column members and bending moment required to cold-straighten them was obtained (Fig. 3). With this information (Eq. (5)) the residual stresses caused by straightening can be estimated.

2. The "modified boring-out method" for the measurement of residual stresses of non-polar symmetric pattern was developed with the use of MacLaurin's expansion method for solving Volterra's integral equation of the first kind. An application of this method to the measurement of the residual stresses in round bars caused by cold-straightening has given fair agreement with the theoretical values obtained by Eq. (5) (Fig. 7c).

3. An approximate but simpler method called the "beam dissection method" was also used for the residual stress measurement. The results were compared with those obtained by the modified boring-out method. Their close correlation indicates the use of the simpler sectioning method for the determination of the residual stresses in solid cylinders (Fig. 8b).

4. In order to confirm the analytical work on the compressive properties of round columns as influenced by the presence of residual stresses due to cold-straightening, stub column tests were carried out on such materials as non-cold-straightened steel, cold-straightened steel and stress-relieved (after cold-straightening) steel. Test results showed a satisfactory correlation with the theoretical prediction of the average stress-strain relationship of short columns (Fig. 9). Furthermore, they indicated that the heat treatment for stress-relieving was quite effective in improving the compressive property (Fig. 10).

5. There exists no bifurcation point in the load-deflection curve of cold-straightened columns which contain anti-symmetric residual stresses. Therefore the tangent modulus concept can not be used for the prediction of their strength. The load-carrying capacity of such columns can be determined by an ultimate load analysis. The strength depends upon both the magnitude of the cold-straightening residual stresses and the out-of-straightness remaining

after the cold-straightening operation. A theoretical analysis on the load-carrying capacity of circular columns was performed. It was found that the ultimate strength of a cold-straightened column ( $d_0 = 0$ ) containing cold-straightened residual stresses with a maximum value approximately one half of  $\sigma_y$  ( $\beta = 0.883$ ), is reduced to about 73% of  $P_y$ , when  $\eta = 1.0$  (Fig. 13). All column test results showed fair agreement with the theoretical predictions of the ultimate strength for both cold-straightened and stress-relieved columns.

### Acknowledgements

This work has been carried out at the Fritz Engineering Laboratory, Lehigh University, Bethlehem, Pennsylvania, in the course of a research project on USS "T-1" constructional alloy steel circular columns sponsored by the United States Steel Corporation.

The authors wish to express their gratitude to Dr. Robert L. Ketter and Dr. Theodore V. Galambos for contributing fruitful discussions and suggestions.

Mr. Dian P. Jen assisted in the testing, in performing the numerical computations and in drawing the figures. His cooperation is gratefully acknowledged.

### Nomenclature

#### Common Notations

Subscripts  $i, j = 1, 2, 3, \dots, N$

#### Functions and Notations

$E$	Young's modulus
$E_t$	Tangent modulus
$F(\zeta)$	Function $= \frac{1}{\cos f^{-1}(\zeta)}$ where $f^{-1}(\zeta)$ is the inverse function of $f(\zeta)$
$F_1(\beta)$	First integral of $F(\zeta)$ , $= \int_{\frac{3\pi}{16}}^{\beta} F(\zeta) d\zeta$
$F_2(\beta)$	Second integral of $F(\zeta)$ , $= \int_{\frac{3\pi}{16}}^{\beta} F_1(\zeta) d\zeta$
$I$	Moment of inertia
$K(\bar{\rho}, \bar{\xi})$	Kernel of integral equations, Eq. (6)
$L$	Length of beam or column
$M$	Bending moment
$M_p$	Full plastic moment
$M_0$	Uniform bending moment

$\bar{M}$	Bending moment associated with a release of residual stress
$N$	Number of division
$P$	Axial thrust
$P_c$	Axial thrust at point $C$ of load-deflection curve (see Fig. 12)
$P_{max}$	Maximum load
$P_y$	Full plastic load ( $= \sigma_y A$ )
$R$	Radius of cross section
$S(\bar{\rho})$	Function obtained by strain measurement $= \frac{\pi}{8} E (1 - \bar{\rho}^2) \bar{\epsilon}(\bar{\rho})$
$U(\lambda, \varphi)$	Axial thrust function $= P/P_y$
$V(\lambda, \varphi)$	Moment function $= \frac{M}{P_y R}$
$X_i(\theta_i)$	Function $= \theta_i - \frac{1}{2} \sin(2\theta_i)$
$Y_i(\theta_i)$	Function $= \sin^3 \theta_i$
$Z_i(\theta_i)$	Function $= \theta_i - \frac{1}{4} \sin(4\theta_i)$
$d$	Deflection of effective column at mid-length
$d_0$	Initial deflection of effective column at mid-length
$f(\theta_0)$	Function $= \frac{3}{8 \cos \theta_0} \left( \frac{\pi}{2} - \theta_0 + \frac{1}{4} \sin 4\theta_0 \right) + \sin^3 \theta$
$k$	Effective column length factor
$l$	Distance between loading point and end of beam
$p$	Concentrated lateral load for cold-bending
$r$	Coordinate (radial direction)
$r_0$	Radius of gyration ( $= R/2$ )
$u(z)$	Lateral deflection of beam or column
$u_e$	Elastic deflection of beam
$u^*$	$= \frac{M_p L^2}{24 EI} (3 - \gamma^2)$
$\bar{u}$	Residual deflection of beam
$x$	Coordinate (in the direction of lateral load, $p$ )
$z$	Coordinate (axial direction)
$z_0$	Boundary between elastic and elastic-plastic region of beam
$\alpha_{ij}$	MacLaurin's coefficients, see Appendix B
$\beta$	Parameter for "cold-straightening of column" $= M_0/M_p$
$\gamma$	Parameter $= \frac{l}{L/2}$
$\delta$	Initial deflection of beam at center (before cold-straightening)
$\epsilon$	Strain (compressive strain is taken positive)
$\epsilon_{ave}$	Average strain
$\epsilon_0$	Symmetric part of strain released by boring-out
$\bar{\epsilon}$	Anti-symmetric part of strain released by boring-out
$\zeta$	Parameter $= \frac{p z}{M_p}$
$\eta$	"Generalized" slenderness ratio $= (k L/r_0) \left( \frac{1}{\pi} \right) \sqrt{\frac{E}{\sigma_y}}$
$\theta_0, \theta_1, \theta_2, \theta_3$	Parameters for elastic-plastic boundary in the cross section

$\lambda$	Parameter $= \frac{\sigma_0}{\sigma_y}$
$\xi$	Non-dimensionalized coordinate $= x/R$
$\bar{\xi}$	Non-dimensionalized coordinate $= (x/R)^2$
$\bar{\rho}$	Non-dimensionalized coordinate $= (r/R)^2$
$\sigma_0$	Stress at the center of cross section as defined by Eq. (41)
$\sigma_r$	Residual stress in radial direction
$\sigma_\theta$	Residual stress in tangential direction
$\sigma_z$	Residual stress in axial direction
$\sigma_y$	Yield stress in simple tension or compression
$\Phi$	Curvature
	Non-dimensional parameter for curvature
$\varphi$	$= \frac{ER}{\sigma_y} \Phi$

## Appendix A

### Deflection Analysis of a Beam With Circular Cross Section

For an elastic-plastic cross section, the internal bending moment,  $M$  and the curvature,  $\Phi$  are given by the following equations:

$$\frac{M}{M_p} = f(\theta_0) = \frac{3}{8 \cos \theta_0} \left( \frac{\pi}{2} - \theta_0 + \frac{1}{4} \sin 4 \theta_0 \right) + \sin^3 \theta_0. \quad (\text{A } 1)$$

$$\frac{\Phi}{\left( \frac{\sigma_y}{ER} \right)} = \frac{1}{\cos \theta_0}. \quad (\text{A } 2)$$

where  $\theta_0$  defines the boundary between the elastic and plastic region in the cross section and  $M_p$  is the full plastic moment of the beam (see Fig. 14).

If  $z = z_0$  is the boundary between the fully elastic part and the elastic-plastic part of the beam shown in Fig. 1, the bending moment due to the load  $p$  is

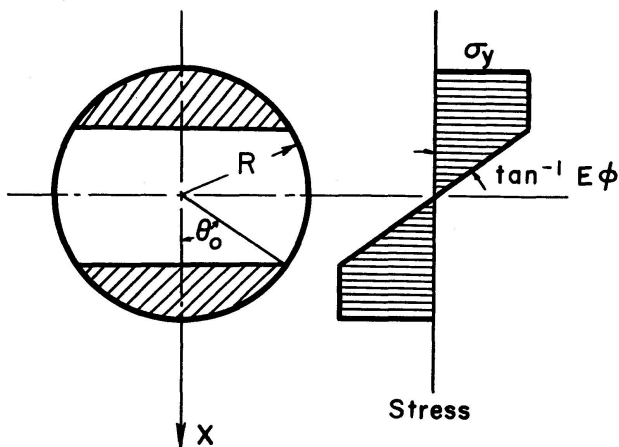


Fig. 14. Cross section of beam.

$$\left. \begin{aligned} M(z) &= pz & \text{(for } 0 \leq z \leq l \text{ )} \\ &= M_0 = pl & \text{(for } l \leq z \leq L/2 \text{ )} \end{aligned} \right\} \quad (\text{A } 3)$$

Since the internal moment  $M$  equals the external one, Eq. (A 1) and Eq. (A 3) lead to

$$z = \frac{M_p}{p} f(\theta_0) \quad (\text{for } z_0 \leq z \leq l). \quad (\text{A } 4)$$

From Eqs. (A 2), (A 3) and (A 4)

$$\begin{aligned} \frac{\Phi}{\left(\frac{\sigma_y}{ER}\right)} &= F(\zeta) & \text{(for } z_0 \leq z \leq l \text{ ),} \\ &= F(\beta) & \text{(for } l \leq z \leq L/2 \text{ ),} \end{aligned} \quad (\text{A } 5)$$

where  $\zeta \equiv \frac{p}{M_p} Z$ ,  $\beta \equiv \frac{M_0}{M_p}$ ,  $F(\zeta) = \frac{1}{\cos[f^{-1}(\zeta)]}$ ,

$f^{-1}(\zeta)$  being the inverse function of  $f(\zeta)$  given by Eq. (A 1).

Then the deflection,  $u$ , of the beam must satisfy the following differential equations:

$$\begin{aligned} \frac{d^2 u}{dz^2} &= -\frac{p}{EI} Z, & \text{(for } 0 \leq z \leq z_0 \text{ ),} \\ &= -\frac{\sigma_y}{ER} F(\zeta), & \text{(for } z_0 \leq z \leq l \text{ ),} \\ &= -\frac{\sigma_y}{ER} F(\beta), & \text{(for } l \leq z \leq L/2 \text{ ).} \end{aligned} \quad (\text{A } 6)$$

With the conditions of continuity for deflection and slope at  $z=z_0$  and  $z=l$ , together with the conditions  $u=0$  at  $z=0$  and  $du/dz=0$  at  $z=L/2$ , the solution for  $u$  will be obtained. Introducing the functions:

$$F_1(\beta) = \int_{\frac{3\pi}{16}}^{\beta} F(\zeta) d\zeta, \quad F_2(\beta) = \int_{\frac{3\pi}{16}}^{\beta} F_1(\zeta) d\zeta,$$

the expression given by Eq. (1) is found.

## Appendix B

### Deduction of the Formula for the “Modified Boring-out Method”

When the specimen is drilled out from the inside up to a radius  $r$ , the bending moment  $\bar{M}(r)$  which is associated with the anti-symmetric residual stress  $\sigma_z(x)$  of the removed part can be expressed in the following equation:

$$\bar{M}(r) = -4 \int_0^r \sigma_z(x) x \sqrt{r^2 - x^2} dx. \quad (\text{B } 1)$$

The remainder of the cross section will be strained by this removal of the stressed material, which, in turn, is equivalent to the application of a moment  $-\bar{M}(r)$  to the specimen inducing a longitudinal strain  $\bar{\epsilon}$  at a distance  $R$  from the neutral axis. Assuming that the ordinary beam theory holds, this concept leads to the following expression:

$$\bar{\epsilon}(r) = -\frac{\bar{M}(r)R}{EI(r)}, \quad (B 2)$$

where

$$I(r) = \frac{\pi}{4}(R^4 - r^4).$$

Using non-dimensional variables, Eqs. (B 1) and (B 2) will result in Eq. (6). Since  $K(\bar{\rho}; \bar{\xi})$  is finite and continuous for any value of  $\bar{\rho}$  and  $\bar{\xi}$ , it is called a regular kernel. Hence this equation can be solved by expanding the right hand term into a mean value of the integral with a division of  $\bar{\rho}$  into  $i$  intervals such that  $\bar{\rho} = i/N$  [6].

$$\begin{aligned} S\left(\frac{i}{N}\right) &= \int_0^{\frac{i}{N}} \sigma_z(\bar{\xi}) K\left(\frac{i}{N}; \bar{\xi}\right) d\bar{\xi} = \sum_{j=1}^i \alpha_{ij} \sigma_z\left(j - \frac{1}{2}, \frac{1}{N}\right) K\left(\frac{i}{N}; j - \frac{1}{2}, \frac{1}{N}\right) \left(\frac{i}{N}\right) = \\ &= \left(\frac{i}{N}\right) \sum_{j=1}^{i-1} \alpha_{ij} \sigma_z\left(j - \frac{1}{2}, \frac{1}{N}\right) K\left(\frac{i}{N}; j - \frac{1}{2}, \frac{1}{N}\right) \\ &\quad + \left(\frac{i}{N}\right) \alpha_{ii} \sigma_z\left(i - \frac{1}{2}, \frac{1}{N}\right) K\left(\frac{i}{N}; i - \frac{1}{2}, \frac{1}{N}\right). \end{aligned} \quad (B 3)$$

This leads to Eq. (7), and the coefficients  $\alpha_{ij}$ 's are listed in Table 2.

Table 2

i	j				
	1	2	3	4	5
1	1	—	—	—	—
2	1/2	1/2	—	—	—
3	3/8	2/8	3/8	—	—
4	13/48	11/48	11/48	13/48	—
5	275/1152	100/1152	402/1152	100/1152	275/1152

### References

1. HUBER, A. W., Residual Stress and the Compressive Properties of Steel, Fritz Laboratory Report No. 220A.22, Lehigh University, May, 1956 (Ph. D. Dissertation).
2. LAMBERT, J. W. A Method of Deriving Residual Stress Equations, Proceedings of the Society for Experimental Stress Analysis, Vol. 12, No. 1, pp. 91—96 (1954).
3. NITTA, A. and THÜRLIMANN, B., Ultimate Strength of High Yield Strength Construc-

tional-Alloy Circular Columns — Effect of Thermal Residual Stresses, International Association for Bridge and Structural Engineering, Publications, Vol. 22 (1962).

4. PRAGER, W. and HODGE, P. G., Jr., Theory of Perfectly Plastic Solids, p. 44, John Wiley & Sons, Inc., New York, 1951.
5. NITTA, A. and THÜRLIMANN, B. Effect of Cold Bending on Column Strength, Fritz Laboratory Report No. 272.2, Lehigh University (July, 1960).
6. HIDAKA, K., Theory of Integral Equations, p. 167, Kawade, Tokyo, 1941.

### Summary

The purpose of this study is to investigate the effect of cold-straightening on the ultimate strength of round column members. Controlled cold-bending tests were first performed simulating the actual straightening operation in mill practice. The resulting residual stresses were then measured by both the "modified boring-out method" and the "beam-dissection method". Stub column rests indicated the influence of these residual stresses on the average compressive properties and proved the effectiveness of stress-relieving. A theoretical analysis on the ultimate load-carrying capacity of circular columns containing residual stresses due to cold straightening (anti-symmetric distribution pattern) was developed. Full-size column tests verified the theoretical predictions.

### Résumé

Les auteurs se proposent d'examiner l'influence du dressage à froid sur la résistance limite des barres circulaires comprimées. On a d'abord exécuté des essais contrôlés de flexion à froid, simulant l'opération réelle de dressage pratiquée en usine. Les contraintes résiduelles résultantes ont ensuite été mesurées par deux méthodes: «la méthode de trépanation modifiée» et «la méthode de débitage». Des essais sur des tronçons de barres ont montré l'influence de ces contraintes sur les propriétés moyennes à la compression et prouvé l'efficacité du recuit de détente. Une analyse théorique de la charge de compression limite des barres circulaires ayant des contraintes résiduelles dues au dressage à froid (distribution anti-symétrique) a été développée. Des essais grandeur nature ont vérifié les indications théoriques.

### Zusammenfassung

Das Ziel der Arbeit ist eine Abklärung des Einflusses von Kalt-Richten von Säulen auf ihre Tragfähigkeit. Zuerst wurden kontrollierte Biegeversuche ausgeführt, um das fabrikmäßige Kalt-Richten nachzuahmen. Die daraus resultierenden Eigenspannungen wurden mittels der «modifizierten Ausbohrungs-

Methode» und der «Streifen-Zerlegungs-Methode» experimentell gemessen. Druckversuche an kurzen Versuchsstücken zeigten den Einfluß der Eigenspannungen auf das durchschnittliche Spannungs-Stauchungs-Diagramm. Weiter wurde der günstige Abbau der Eigenspannungen durch Spannungsfrei-Glühen festgestellt. Eine Lösung für die Bruchlast von Säulen mit Kreisquerschnitt unter Berücksichtigung der Eigenspannungen infolge Kalt-Richtens (antisymmetrische Eigenspannungsverteilung) wird entwickelt. Versuche an Säulen bestätigten die theoretischen Resultate.